

See discussions, stats, and author profiles for this publication at: <https://www.researchgate.net/publication/341826642>

# Design and evaluation of a novel nanodrug delivery system for reducing the side effects of clomiphene citrate on endometrium

Article in DARU Journal of Pharmaceutical Sciences · June 2020

DOI: 10.1007/s40199-019-00310-2

CITATION

1

READS

76

7 authors, including:



**Marziyeh Ajdary**

Iran University of Medical Sciences

21 PUBLICATIONS 222 CITATIONS

[SEE PROFILE](#)



**Fariborz Keyhanfar**

Iran University of Medical Sciences

30 PUBLICATIONS 334 CITATIONS

[SEE PROFILE](#)



**Reza Aflatoonian**

Royan Institute

95 PUBLICATIONS 1,179 CITATIONS

[SEE PROFILE](#)



**Amir Amani**

Tehran University of Medical Sciences

123 PUBLICATIONS 1,635 CITATIONS

[SEE PROFILE](#)

Some of the authors of this publication are also working on these related projects:



Anti-inflammatory effects of eugenol nanoemulsion as a topical delivery system [View project](#)



In vitro development of embryos from experimentally Kerack-addicted Mice [View project](#)



# Design and evaluation of a novel nanodrug delivery system for reducing the side effects of clomiphene citrate on endometrium

Marziyeh Ajdary<sup>1</sup> · Fariborz Keyhanfar<sup>2</sup> · Reza Aflatoonian<sup>3</sup> · Amir Amani<sup>4,5</sup> · FatemehSadat Amjadi<sup>6</sup> · Zahra Zandieh<sup>6</sup> · Mehdi Mehdizadeh<sup>1,6</sup>

Received: 20 March 2019 / Accepted: 23 October 2019  
© Springer Nature Switzerland AG 2019

## Abstract

**Background** Stimulation of ovulation with clomiphene citrate can cause side effects on endometrial receptivity. Formulation with nano-size may be an alternative therapy for women with ovulatory disorders. In this study, we investigated sustained-release clomiphene citrate by using Phosal-based formulation (PBF) and evaluate its decreased side effect on the endometrial receptivity.

**Methods** In the in-vitro study, CC loaded PBF was analyzed using Zetasizer, Fourier-transform infrared spectroscopy (FTIR), and Transmission electron microscopy (TEM). In the in-vivo study, 24 female mice were randomly divided into three groups: CC (5 mg/kg), CC/PBF (5 mg/kg) and SS (1 ml) daily administered and injected with 5 IU HCG and mated after two days. At day 4.5, pregnant mice were euthanized and endometrial tissue was extracted for quantitative polymerase chain reaction (Q-PCR) analysis.

**Results** The optimized PBF contained Phosal 50PG/glycerol in a 2:8 ratios (w/w) and the particle size of optimum formulation was  $67 \pm 0.30551$  nm and the release of CC from CC-containing PBF was slightly faster in the first 24 h; wherein, 29% of CC was released, and 76% of CC was released up to 120 h. The mRNA levels of leukemia inhibitory factor (*LIF*), leukemia inhibitory factor receptor alpha (*LIFR*), *HOXA10*, Heparin-binding epidermal growth factor (*HB-EGF*), and epidermal growth factor (*EGF*) were significantly upregulated and *MUC1* and *PGR* mRNA levels were significantly downregulated in the CC-containing PBF-treated animals compared with only CC group ( $P < 0.05$ ).

**Conclusion** Sustained release formulation of clomiphene citrate increased its targeting efficiency and improved the impact of the CC on implantation.

**Keywords** Endometrial receptivity · Clomiphene citrate · Phosal-based formulation · Sustained release

## Introduction

Clomiphene citrate (CC) with the chemical name of 2-[4-[(Z)-2-chloro-1, 2-diphenylethenyl] phenoxy]-N, N-diethylethanamine; 2-hydroxypropane-1, 2, 3-tricarboxylic acid

was used in the first line of pharmacological ovulation induction in ovulation disorders. CC is related to a group of selective estrogen receptor modulators (SERMs) that can be bound to the receptors of estrogen via agonist and antagonist functions in cervical mucus and endometrium [1, 2]. However, CC has

✉ Mehdi Mehdizadeh  
mehdizadeh.m@iums.ac.ir

<sup>1</sup> Cellular and Molecular Research Center, Iran University of Medical Sciences, Tehran, Iran

<sup>2</sup> Department of Pharmacology, School of Medicine, Iran University of Medical Sciences, Tehran, Iran

<sup>3</sup> Department of Endocrinology and Female Infertility, Reproductive Biomedicine Research Center, Royan Institute for Reproductive Biomedicine, ACECR, Tehran, Iran

<sup>4</sup> Natural Products and Medicinal Plants Research Center, North Khorasan University of Medical Sciences, Bojnurd, Iran

<sup>5</sup> Department of Medical Nanotechnology, School of Advanced Technologies in Medicine, Tehran University of Medical Sciences, Tehran, Iran

<sup>6</sup> Department of Anatomical Science, Iran University of Medical Sciences, Tehran, Iran

various side effects, such as anti-estrogenic action on the endometrium, and CC can also potentially suppress endometrial receptivity [3].

Implantation is associated with alteration in the expression of genes that affect embryonic and endometrial interactions, and any change in the expression of these genes will lead to implantation failure and ultimately infertility [4].

Recent studies showed that the formulations for sustained-release drug delivery systems (SRDDSs) are expected to achieve sustained release rates, decrease the number of daily administrations, improve compliance, and minimize the side effects. At this point, it has been suggested that the formulations, which sustain the release of CC, have been quite effective [5]. Previous studies have revealed that phospholipids (one of the main components of Phosal-Based Formulation (PBF)) can be used for enhancing drug efficacy and reducing the total dose required, quick onset of action, comfort preparation and scale-up, reduced side effects and drug protection against hydrolysis. Also, phospholipids protect the drugs from degradation in the gastrointestinal tract [6]. Phosal 50PG is another compound used in some lipid-based formulations to improve the absorption, effectiveness, decrease side effects, and therapeutic index of the active ingredients [7, 8]. This formulation ultimately results in the formation of transparency of a translucent water-soluble concentrate with a particle size of approximately 100 nm [9]. To decrease the side effects of CC, we tried to exhibit a new CC-containing PBF. Subsequently, the decreased side effects of CC and pharmacokinetic parameters of CC-containing PBF were examined in female mice.

## Materials and methods

### Materials

Clomiphene citrate (internal standard) was purchased from Iran Hormone Pharmaceutical Co. (Tehran, Iran). Phosal 53 medium-chain triglyceride (MCT) was a kind gift from Lipoid GmbH (Ludwigshafen, Germany). Glycerol and TRIZOL were purchased from Sigma Aldrich Merck (St. Louis, MI, USA). Deionized water was obtained from a Milli-Q water purification system (Millipore, Burlington, MA, USA). SYBR Premix Ex Taq was purchased from Applied Biosystems (Foster City, CA, USA), and cDNA synthesis kits were purchased from Thermo Fisher Scientific (Waltham, MA, USA).

### In-vitro studies

#### Preparation of PBF

A serial dilution of formulations was prepared with different weight ratios of Phosal 50PG and glycerol in the range of 1:9 to 9:1. A consistent amount of CC was dissolved in Phosal

50PG for all formulations before glycerol was added. This mixture was homogenized for 10 min. After the addition of water, the mixture was vortexed and sonicated using a probe sonicator for 10 min. The mixture was stored at room temperature until the next usage. The compositions of difference PBFs have been presented in Table 1 [10].

The optimized PBF contained Phosal 50PG/glycerol was selected in a 2:8 ratio (w/w) for its stability test, which includes centrifuge tests, heating/cooling, and freeze/thaw cycles. The protocol of these three tests was as follows: CC/PBF solution was centrifuged at a round of 5000×g for 30 min and no separation was performed, and if no two-phase separation was seen, it was selected to test for heating/cooling and freeze/thaw cycles. During the heating/cooling cycles, the samples were incubated in 6 rounds at 4 °C and 45 °C for 48 h and their stability was evaluated. During the freeze/thaw cycle, it was performed three times for 48 h at −21 °C and +25 °C, and all instability symptoms, including phase separation, were investigated.

### Physicochemical properties of CC-containing PBF

The final formulations were diluted 50, 100, 500, and 1000 times with distilled water to assess visually any phase separation or drug precipitation immediately; this procedure was repeated after three months. A UV–visible spectrophotometer (Pharmacia Biotech, England) was used to determine the transparency of the formulations. Percent transmittance of formulations diluted 200 times in double distilled water was measured at 650 nm using double distilled water as blank [10].

The mean droplet sizes and polydispersity indices (PDI) of the formulations were measured using dynamic light scattering by a Zetasizer Nano (Malvern Panalytical, UK) at an angle of 90° to measure the Brownian motion; in addition, the size of the particles was determined by illuminating the particles with a laser and analyzing the intensity of the fluctuations in the scattered light [11]. The formulation (50 µL) was diluted to 5 mL with double distilled water to prevent the particle interactions and extra scattering during determination. The dispersant viscosity was set at 0.8872 cP at 25 °C. In order to calculate the zeta potential of formulation (50 µL), it was diluted 100 times with double distilled water. This potential

**Table 1** Composition of various Phosal-Based Formulations

Ingredient	Formulations								
	F1	F2	F3	F4	F5	F6	F7	F8	F9
Phosal 50 PG (mg)	100	200	300	400	500	600	700	800	900
Glycerol (mg)	900	800	700	600	500	400	300	200	100
CC (mg)	5	5	5	5	5	5	5	5	5
Water (mL)	5	5	5	5	5	5	5	5	5

was determined by Zetasizer Nano through considering the electrophoretic mobility and afterward using the Henry eq. A transmission electron microscopy (TEM) was used to investigate the morphological and structural features of CC-containing PBF. Samples (50  $\mu\text{L}$ ) of the diluted formulations were added to a 200-mesh film grid and dried at room temperature. A TEM microscope was applied to view the stained samples with uranyl acetate (ZEISS, Oberkochen, Germany). The infrared spectra of CC-loaded PBF, CC and PBF were captured by a Fourier Transform-Infrared Spectroscopy (PerkinElmer, Waltham, MA, USA). The spectra of all the materials were recorded at a frequency range averaged over four runs. The powdered samples were placed on the attenuated total reflectance crystal and then compressed using an axial screw.

### Evaluation of drug release from CC-containing PBF in its release environment

The procedure for performing a standard curve on CC requires that dilutions be made from a 20 mg stock standard solution. A four-point curve is generally used with concentrations of 2.5, 5, 10, and 15 mg in 1 mL dimethylformamide. Experiments were performed spectrophotometrically at 460 nm with three replicates for each concentration for investigating the in-vitro release of CC from CC-containing PBF. Five milligrams of CC-containing PBF was added in 5 mL of phosphate-buffered saline (PBS); pH 7.4, and the suspension was incubated at 37 °C. The tubes were centrifuged and the supernatants were extracted for the determination of CC, which was evaluated by a UV–visible spectrophotometer through a study of the absorption peak at 460 nm. Then, the supernatants were substituted by the equal amount of fresh PBS solution and the tubes were then located again in the incubator.

### In-vivo experiments

#### Animals

Twenty-four female and 12 male mice weighing 20–50 g at 8 weeks of age were obtained from the Pasteur Institute and maintained at  $25 \pm 0.5$  °C, 60–80% humidity, and maintained in a 12 h light/dark cycle. It should be noted that food and water were also kept in the mentioned controlled condition. Vaginal smears were evaluated every day and mice showing just two successive estrous cycles were considered in the experiments. All experiments were done following the National Institutes of Health Guide for the Care and Use of Laboratory Animals (NIH Publication No. 80–23, revised 1996) and were approved by the Research and Ethics Committee of Iran University of Medical Sciences, Iran, (IR-IUMS.1394.94–05–117–27,524).

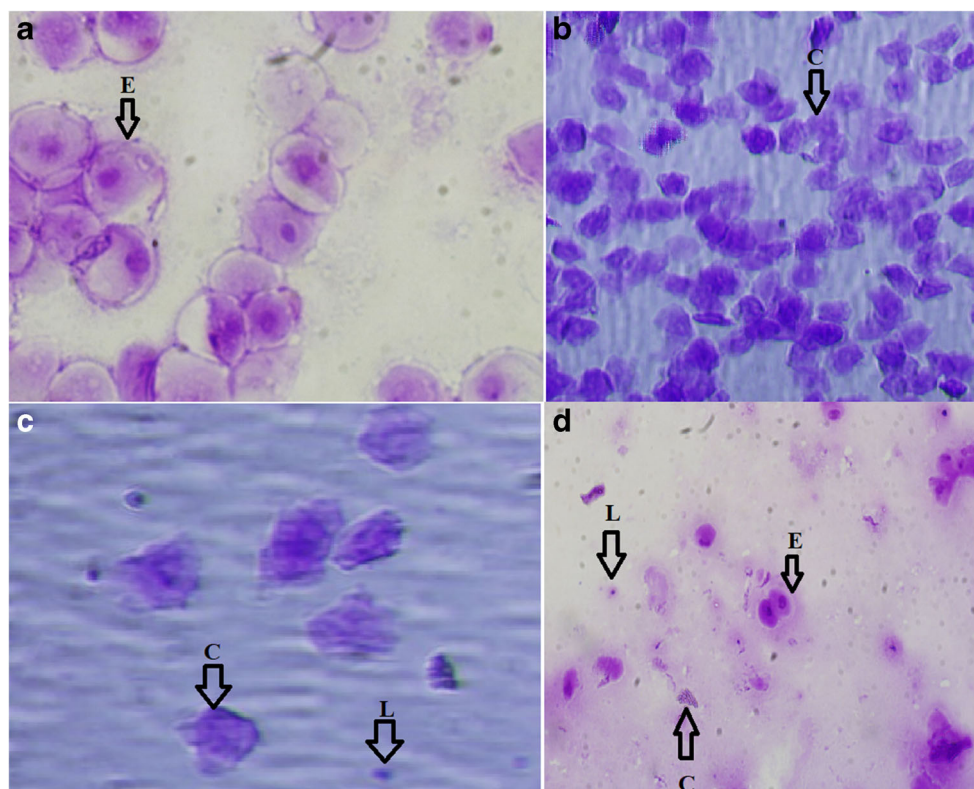
### Ovarian stimulation

All the female mice were divided into three groups: normal saline solution (SS), CC-containing PBF, and CC. The dose received was based on previous studies [12, 13]. The stage of the estrous cycle was determined by microscopic analysis of the predominant cell type in vaginal smears (Fig. 1). In the proestrus step, mice have orally directed CC-containing (5 mg/kg), CC/PBF and SS (1 ml) daily for two days. All the female mice were injected with human chorionic gonadotropin (HCG) 5 IU (Lizhu Pharmaceutical Co., China) at 05:00 pm two days later and then they were coupled with a sexually mature male mouse [14]. The vaginal plugs were investigated at the next morning and this day was called gestation day 1. Besides, the pregnant animals were killed with ether on day 4.5, and the endometrial tissues were collected and frozen in liquid nitrogen and stored at  $-80$  °C for RNA extraction. Blood serum was separated from the collected blood by centrifugation at  $4000 \times g$  for 10 min. The serum samples were stored in a deep freezer at  $-20$  °C. The blood estradiol (E2) concentrations were measured by the Testosterone ELISA kit (Catalog no. ab108666, Abcam, Cambridge, UK) [15].

### Reverse transcription-polymerase chain reaction (RT-PCR) analysis

Based on materials using criteria, the whole RNA was purified from the endometrial samples via homogenization in 1 mL of TRIzol Substance (Merck, USA). Technical replicates were followed for all samples in triplicates. All participates were incubated with DNase I to eliminate the genomic DNA adulteration (IPTG, MBI Fermentas GmbH, St. Leon-Rot, Germany). In order to specify the RNA concentration (yield and purity), the samples were analyzed spectrophotometrically by the A260/A280 ratio technique. Superscript First-Strand synthesis system (200 U/mL, Invitrogen, Carlsbad, CA, USA) and oligo dT primers (Metabion, Martinsried, Germany) were used to reverse-transcription of total RNA. In each PCR cycle, a reverse transcription control was performed using the conditions mentioned before without superscript II enzyme. In the initial investigations, the primer pairs were evaluated via a conventional PCR protocol (Invitrogen), and the products run on an agarose gel and confined to a single band of the expected size. As the endogenous control, quantitative RT-PCR was applied to determine the mRNA transcript concentrations of *EGF*, *HOXA10*, *PGR*, *MUC1*, *Colony-stimulating factor (CSF1)*, *HBEGF*, *LIFR*, *LIF*, *Fibroblast growth factor-2 (FGF2)* and *Vascular endothelial growth factor A (VEGFA)*, with  $\beta$ -*ACTIN* transcript concentrations. The applied gene-specific primers have been detailed in Table 2. Negative controls (no cDNA) were considered for all experiments. The qPCR reactions were performed based on the mentioned details formerly [16]. The qPCR data were analyzed via the  $C_T$  method [16].

**Fig. 1** Cytological assessment of vaginal smears can be used to identify the estrous stage. Three main cell types were detected in vaginal smear samples: (E) nucleated epithelial cells, (C) cornified squamous epithelial cells, and (L) leukocytes. The ratio of these cell types present in the smear can be used to identify mice in (A) proestrus, (B) estrus, (C) metestrus, or (D) diestrus as described in representative results (Scale bars = 50  $\mu$ m)



## Statistical analyses

All data presented as the mean  $\pm$  SEM. The statistical significance of differences between the groups was determined using one-way analysis of variance (ANOVA), followed by Tukey's post hoc test. Statistical Package for the Social Sciences (SPSS version 16.0, SPSS Inc., Chicago, IL, USA) was used for all data analyses. A value of  $P < 0.05$  was considered statistically significant.

## Results

### Preparation and characterization of formulation

A new formulation using Phosal 50PG, as an easy-to-use carrier for lipophilic compounds, was prepared in glycerol. The results of the droplet size analysis revealed that the differences in the weight ratio of Phosal 50PG and glycerol did not affect the mean globule size of the formulations considerably (Fig. 2a). Among these ratios (w/w), F2 (Phosal/glycerol = 2:8) was selected for the subsequent experiments. In addition to the particle size, other factors, such as maintenance of a suitable viscosity after diluting with a constant amount of water (administered orally in mice), stability against creaming and phase separation, and the presence

of an adequate amount of Phosal 50PG to solubilize the determined dose (5 mg/kg), were considered during the selection of the optimal formulation.

### Thermodynamic stability analysis

The results of the stability experiments for the freeze-thaw cycles, heating-cooling cycles and CC-containing PBF included centrifugation analysis were evaluated for the selected formulations from F2 (Table 3).

The only formula (F2 (Phosal/glycerol = 2: 8)) that remained stable under centrifuging, freeze/thawing and heating/cooling conditions, and was not two-phase and showed the optimum thermodynamic stability, selected for further experiments.

The size analysis for the first day and after the third month of preparation was followed via the stability tests of formulations (Table 4). According to the particle size analysis, sample F2 with minimal alteration in the particle size was considered as the optimal sample for additional examinations. The low PDI also approved the homogeneity of droplets.

### Physicochemical characterization of CC/ PBF

Differential light scattering (DLS) analysis showed that the CC-containing PBF had a mean hydrodynamic diameter of

**Table 2** The sequence of the primers used in the current investigation

Gene		Sequence (5' -> 3')	Length	Tm	GC%	Self-complementarity	Self-3' complementarity
Mucin 1, cell surface associated ( <i>MUC1</i> )	Forward primer	TAGCATCAAGTTCAGGTCAGGC	22	60.36	50.00	3.00	2.00
	Reverse primer	GACTTCACGTCAGAGGCACTAA	22	60.03	50.00	5.00	3.00
Epidermal growth factor ( <i>EGF</i> )	Forward primer	ACTGGACGGTTTGCCTCTTT	20	59.82	50.00	3.00	0.00
	Reverse primer	ATTCAGGGGTTGACAGAGCAT	21	59.36	47.62	3.00	2.00
Heparin-binding EGF-like growth factor ( <i>HBEGF</i> )	Forward primer	CCCAGAAGAGATTGAGCATCCA	22	59.83	50.00	3.00	2.00
	Reverse primer	ACCCGAAGAACAGCAGGATAAG	22	60.09	50.00	2.00	0.00
Fibroblast growth factor-2 ( <i>FGF2</i> )	Forward primer	GACCCACACGTCAAACACTACAAC	22	59.71	50.00	4.00	0.00
	Reverse primer	CTGTAACACACTTAGAAGCCAGC	23	59.57	47.83	5.00	2.00
Homeobox gene 10 ( <i>HOXA10</i> )	Forward primer	TGTTTAATCAGGGAGTCCAGGC	22	60.03	50.00	6.00	2.00
	Reverse primer	TTTTCAACCAGCCAGGTCAAG	22	59.57	45.45	5.00	1.00
Colony stimulating factor ( <i>CSF1</i> )	Forward primer	GGCATCATCCTAGTCTTGCTGA	22	59.90	50.00	4.00	3.00
	Reverse primer	AATCCAATGTCTGAGGGTCTCG	22	59.83	50.00	3.00	2.00
Leukemia inhibitory factor ( <i>LIF</i> )	Forward primer	TTCCAGGTACTIONACTGCACTC	22	59.96	50.00	4.00	2.00
	Reverse primer	TCTCAGACCAACACCCCTATTG	22	59.96	50.00	5.00	3.00
Leukemia inhibitory factor receptor alpha ( <i>LIFR</i> )	Forward primer	TGTCTGCTGACTTCTTCACCTC	22	59.96	50.00	6.00	0.00
	Reverse primer	TAACACGAGTGCTACTGGTTCC	22	60.03	50.00	6.00	2.00
Progesterone receptor ( <i>PGR</i> )	Forward primer	AAAAGTCCCAGCATGTCTGT	20	60.82	50.00	4.00	1.00
	Reverse primer	CAACACCGTCAAGGGTCTCAT	22	60.81	50.00	5.00	2.00
Vascular endothelial growth factor A ( <i>VEGFA</i> )	Forward primer	TGCAGATTATGCGGATCAAACC	22	59.38	45.45	5.00	2.00
	Reverse primer	TGCATTACATTGTTGTGCTGTAG	22	61.02	40.00	4.00	2.00
Actin, beta ( $\beta$ -actin)	Forward primer	CAAGATCATTGCTCCTCCTG	20	58.4	50.00	6.00	1.00
	Reverse primer	ATCCACATCTGCTGGAAGG	19	57.3	52.60	6.00	0.00

$67 \pm 0.30551$  nm and zeta potential (mV) was in the range of  $-2.2 \pm 0.14$ , and the transmittance was in the range of  $80.8 \pm 0.31$  (Fig. 2b). The spherical structure of CC-containing PBF samples was obtained through TEM micrographs with the particle size of 126–250 nm. It should be noted that this size was reliable against DLS investigations (Fig. 2c). The conjugated PBF NPs with Phosal 50PG and the loaded drug were approved by FT-IR analysis where the creation of the amide bond following conjugation was found in the peaks at  $1043,993 \text{ cm}^{-1}$  in Phosal 50PG to PBF NPs evidently (Fig. 2d). The presence of the drug in NPs has been confirmed in CC-loaded NPs via the found peaks at 695 and  $669 \text{ cm}^{-1}$ . It may be considered that at the concentrations of 2.5–15 mg/ml the linearity of the drug response was approved. The calibration curve was obtained by plotting the absorbance versus the concentration data and checked for linear regression. The equation of the calibration curve for CC obtained was  $Y = 0.218 + 0.024X$ , and the calibration curve was found to be linear in the aforementioned concentrations (the correlation coefficient,  $r^2$  of determination was 0.166) (Fig. 2e). The release of CC from PBF was determined in a PBS release medium with a pH of 7.4 at  $37^\circ\text{C}$ . The drug release was examined for 7 days. The resulting curves showed an initial rapid release phase followed by a

slower, continuous-release phase during the next 7 days (Fig. 2f). Releasing CC from CC-containing PBF during the first 24, 48, 72 and 96 h was 29%, 58%, 70%, and 75%, respectively. Afterward, a Plateau is observed in the release pattern.

The first point when the drug release reached plateau was 96 h. The drug release was then checked for sure. The time required for the injection of the drug, which was proestrus and estrus, was two days; in addition, given that the drug release rate was 58% in the next 48 h, it was actually 2.9 mg/kg, and previous studies have suggested a suitable dose for ovulation to induce maximum implantation in the range of 2.5–3 mg/kg [17, 18].

### Determination of loading efficiency of the CC

In determining the amount of drug in PBF, an UV-visible spectrophotometer was used (model UV-1650 PC; Shimadzu Europe, Tokyo, Japan). 5 mg of CC-containing PBF was added to 1 mL Dichloromethane (DCM) followed by the addition of 1 mL PBS (pH 7.4) and centrifuged at 11,200 rcf for 20 mins. Drug loading was determined at 460 nm using the UV-visible spectrophotometer and the obtained data was compared with the previously established standard curve. The concentration of CC was determined using Beer's law (Fig. 2g).

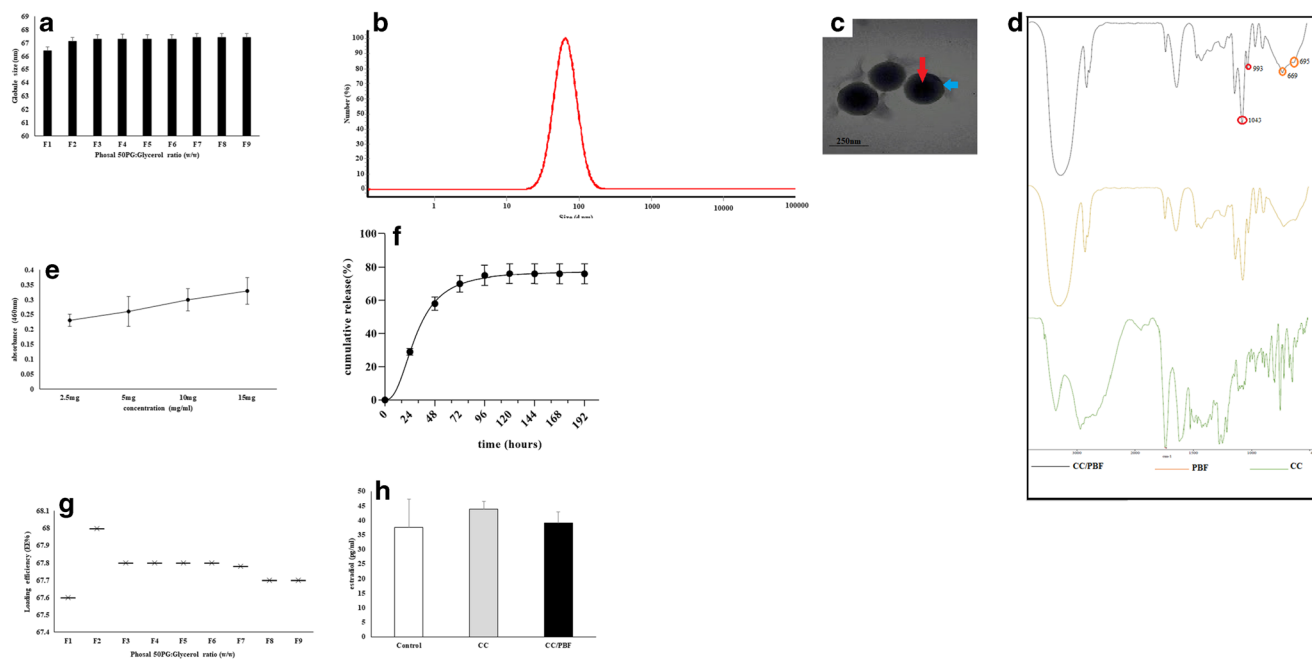


**Fig. 2** Physicochemical characterization of CC-containing PBF: (a) the effect of Phosal 50PG: glycerol ratio (*w/w*) on the mean globule size of various CC- containing PBF formulations (F1 to F9). Data are represented as the mean ± SEM (*n* = 3); (b) Size of the CC-containing PBF was determined by DLS; (c) TEM micrograph of spherical-shaped CC-loaded PBF (bar: 250 nm). The red arrows represent a completely dark center and the blue arrows show the bright margin of the

nanoparticle, indicating the loaded drug and the environmental PBF; (d) FT-IR spectrum of CC/PBF; (e) Calibration curve for the release of the CC-loaded PBF; (f) Sustained-release phenomenon exhibited by CC-loaded PBF in PBS with pH of 7.4 at 37 °C; (g) Determination of loading efficiency of CC; (h) Effects of CC and CC-containing PBF on serum reproductive hormone levels in NMRI mice. Data are expressed as the mean ± SEM

The highest loading efficiency (68%) was related to the F2 formula (Phosal / glycerol = 2: 8), which showed a better loading capacity.

Encapsulation efficiency (EE) (%)

$$= \frac{\text{Amount of encapsulated clomiphen citrate (mg) in nanocapsule}}{\text{Initial amount of clomiphen citrate (mg) used in the recipe}} \times 100$$

**Table 3** Thermodynamic stability test of various Phosal-Based Formulations

An observation based on the thermodynamic stability study

Ingredient	H/C	Cent	Freez/thaw
F1	×	✓	✓
F2	✓	✓	✓
F3	✓	✓	×
F4	×	✓	✓
F5	×	✓	✓
F6	×	✓	×
F7	✓	✓	×
F8	✓	✓	×
F9	×	✓	×

H/C: Heating-cooling cycle; Cent: Centrifugation; Freez/Tha: Freeze-thaw cycle. ✓: Passed; ×: Failed

### Hormonal assessment

As shown in Fig. 2h, the mean serum levels of E2 were higher in the CC-administered animals against animals in the SS groups ( $43.82 \pm 2.64$  vs.  $37.5 \pm 9.69$ ,  $P = 0.77$ ). However, the mean serum levels of E2 were not changed significantly in the CC-containing PBF-administered animals compared to SS groups ( $39.02 \pm 3.9$  vs.  $37.5 \pm 9.69$ ,  $P = 0.98$ ) and the mean serum levels of E2 were higher in the CC-administered animals against animals in the CC-containing PBF groups ( $43.82 \pm 2.64$  vs.  $39.02 \pm 3.9$ ,  $P = 0.85$ ).

### Gene expression in endometrial tissues

The mean mRNA levels of *LIF*, *LIFR*, *HOXA10*, *CSF*, *HBEGF* and *EGF* in the CC-administered group were significantly lower against SS and CC-containing PBF-administered groups ( $P < 0.05$ ). However, the mean mRNA levels of *CSF*, *vascular endothelial growth factor (VEGF)*, and *FGF2* were not different significantly in the CC group compared to the SS and CC-containing PBF groups. The mean mRNA levels of *MUC1* and *PGR* were significantly higher in the CC group against SS and CC-containing PBF groups ( $P < 0.05$ ; Fig. 3, Table 5).

**Table 4** Composition, droplet size, and polydispersity index (PDI) of selected clomiphene citrate containing PBF

Ingredient	Mean droplet size $\pm$ S.D. (nm)		P value	PDI $\pm$ S.D		P value
	Day 1	Month 3		Day 1	Month 3	
F1	67.5 $\pm$ 0.20660	77 $\pm$ 0.40220	0.0001	0.36 $\pm$ 0.03	0.37 $\pm$ 0.05	>0.9999
F2	67 $\pm$ 0.30551	72 $\pm$ 0.50102	>0.9999	0.26 $\pm$ 0.08	0.30 $\pm$ 0.03	>0.9999
F3	67.3 $\pm$ 0.30551	73 $\pm$ 0.60221	0.001	0.36 $\pm$ 0.04	0.45 $\pm$ 0.10	0.0001
F4	68 $\pm$ 0.40441	80 $\pm$ 0.60341	0.0001	0.37 $\pm$ 0.07	0.45 $\pm$ 0.10	0.0001
F5	68 $\pm$ 0.40441	80 $\pm$ 0.60341	0.0001	0.37 $\pm$ 0.07	0.45 $\pm$ 0.10	0.0001
F6	68 $\pm$ 0.40441	82 $\pm$ 0.20551	0.0001	0.37 $\pm$ 0.07	0.45 $\pm$ 0.10	0.0001
F7	69 $\pm$ 0.50447	82 $\pm$ 0.20551	0.0001	0.39 $\pm$ 0.04	0.5 $\pm$ 0.11	0.0001
F8	69 $\pm$ 0.50447	82 $\pm$ 0.20551	0.0001	0.39 $\pm$ 0.04	0.5 $\pm$ 0.11	0.0001
F9	69 $\pm$ 0.50447	82 $\pm$ 0.20551	0.0001	0.39 $\pm$ 0.04	0.5 $\pm$ 0.11	0.0001

## Discussion

Ovulation disorder is the most common cause of clomiphene citrate use in women undergoing IVF. Clomiphene citrate is one of the selective estrogen receptor modulator drugs (SERMs) and acts on the estrogen receptor with both estrogen agonist and antagonistic effects in other tissues [19].

Many studies have shown that stimulation of ovulation by CC induces reduced endometrial receptivity, but its undesirable effects can lead to the reduced successful embryo implantation serious complications during implantation [20].

In this research, a hypothesis that encapsulation of the clomiphene citrate lipid drug in PBF can reduce its effects on non-target tissues and increase the therapeutic effect as well as improving the pharmacological properties has been proposed.

Our results showed that endometrial expression of *LIF*, *LIFR*, *HOXA10*, *HBEGF*, and *EGF* mRNA were upregulated and endometrial *MUC1* and *PGR* mRNA levels were down-regulated in the CC-containing PBF-treated animals compared with the CC group. This data confirmed that CC/PBF showed low side effects on implantation.

Given these results, the encapsulated drug in PBF and the reduced particle size reduced damage to endometrial tissue and improved implantation; in fact, it has been one of the factors contributing to increasing the implant size.

The drug is loaded onto the particle surface when the nano-particle size is higher, and, the drug is loaded into the oil core when the particle size is smaller, for this same reason, by measuring the particle size by DLS and zeta potential we concluded that the lower particle size causes the higher particle stability. Also, previous studies showed that when the particle size decreases, bioavailability and remained in blood circulation for a long time will be increased [21]. In this study, the optimum formula (2: 8 ratios (w/w)) was 67  $\pm$  0.30551 nm, which resulted in a higher blood stability rate and slower drug release rate and this slow release of the drug reduced clomiphene citrate damage to the endometrial tissue. Previous studies have shown that the nano particulate drug delivery system improves efficacy by lowering IC50 and also due to drug protection from macrophage cells prolongs a higher blood stability rate and slows the drug release rate [22] and also cause the good stability during storage at room temperature and 4 °C. It has been indicated that sometimes it is not possible

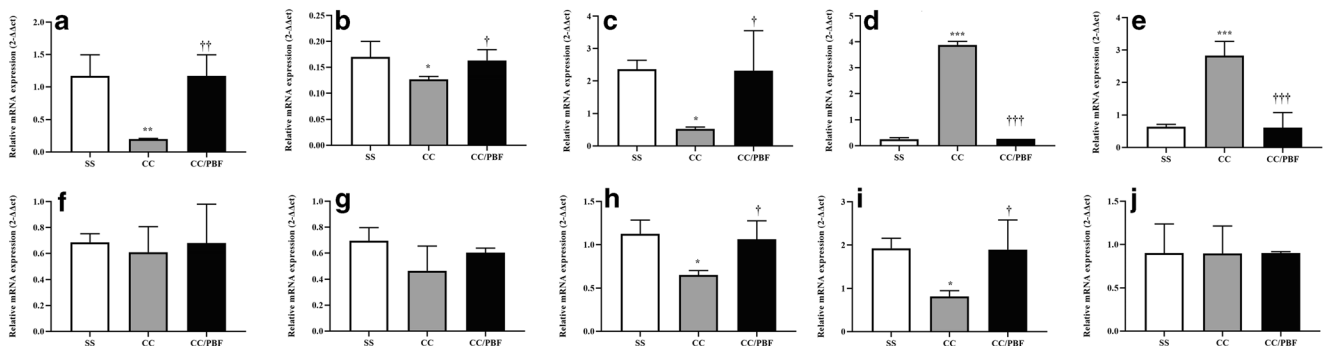


**Fig. 3** Gene expression in endometrial tissues from pregnant mice stimulated with CC, CC-containing PBF, and SS. The mRNA levels were evaluated by qRT-PCR. Data are represented as mean  $\pm$  SEM ( $n = 6$  each group).  $\beta$ -actin was used as an internal control. (a) *LIF*, (b) *LIFR*,

(c) *HOXA10*, (d) *MUC1*, (e) *PGR*, (f) *CSF*, (g) *VEGF*, (h) *HBEGF*, (i) *EGF*, (j) *FGF2*. \* $P < 0.05$ , \*\* $P < 0.01$ , and \*\*\* $P < 0.001$ . \*the comparison was made between CC group vs. SS groups, † The comparison was made between CC-containing PBF group vs. CC groups



**Table 5** Gene expression in endometrial tissues from pregnant mice stimulated with CC, CC-containing PBF, and SS

Gene name	Normal saline solution (mean $\pm$ SEM)	Clomiphene citrate (mean $\pm$ SEM)	Clomiphene citrate containing PBF (mean $\pm$ SEM)	<i>P</i> value
LIF	1.17 $\pm$ 0.19	0.20 $\pm$ 0.01	1.17 $\pm$ 0.19	$P_1 = 0.01, P_2 = 0.01, P_3 = 1.00$
LIFR	0.17 $\pm$ 0.01	0.11 $\pm$ 0.0031	0.16 $\pm$ 0.010	$P_1 = 0.02, P_2 = 0.04, P_3 = 0.70$
HOXA10	2.36 $\pm$ 0.15	0.52 $\pm$ 0.03	0.23 $\pm$ 0.71	$P_1 = 0.04, P_2 = 0.05, P_3 = 0.98$
MUC1	0.24 $\pm$ 0.03	3.88 $\pm$ 0.08	0.26 $\pm$ 0.0004	$P_1 = 0.001, P_2 = 0.001, P_3 = 0.95$
PGR	0.64 $\pm$ 0.04	2.82 $\pm$ 0.25	0.61 $\pm$ 0.26	$P_1 = 0.001, P_2 = 0.001, P_3 = 0.99$
CSF	0.69 $\pm$ 0.03	0.61 $\pm$ 0.10	0.67 $\pm$ 0.17	$P_1 = 0.89, P_2 = 0.92, P_3 = 0.98$
VEGF	0.69 $\pm$ 0.05	0.46 $\pm$ 0.11	0.60 $\pm$ 0.018	$P_1 = 0.14, P_2 = 0.42, P_3 = 0.66$
HBEGF	1.13 $\pm$ 0.09	0.65 $\pm$ 0.031	1.06 $\pm$ 0.12	$P_1 = 0.03, P_2 = 0.04, P_3 = 0.86$
EGF	1.92 $\pm$ 0.13	0.81 $\pm$ 0.080	1.89 $\pm$ 0.39	$P_1 = 0.04, P_2 = 0.04, P_3 = 0.99$
FGF2	0.90 $\pm$ 0.19	0.89 $\pm$ 0.18	0.90 $\pm$ 0.01	$P_1 = 1.00, P_2 = 1.00, P_3 = 1.00$

$P_1$ : The comparison was performed between CC and SS groups,  $P_2$ : The comparison was performed between CC-containing PBF vs. CC groups,  $P_3$ : The comparison was performed between CC-containing PBF and SS groups. All data have been presented as the mean  $\pm$  SEM. The statistical significance of differences between the groups was determined using one-way analysis of variance (ANOVA), followed by Tukey's post hoc test

to predict the stability of a formulation based solely on the zeta potential values, because the electrostatic stabilization may not be the main mechanism for the stability of these formulations [8]. The presence of the solvated drugs in nano lipid globules (<150 nm) decreased the observed side effects. The droplet size is a very important characteristic because the rate and extent of drug release and absorption are dependent on it [11].

Polyols have been shown to have some remarkable advantages compared with water as a continuous phase in the field of oil-water solution. The influence of interface between oil and polyol/water leads to reduced interfacial tension and hence lower diameters of the oil droplets are observed compared with a pure water phase. The presence of the polyglycols in Phosal 50PG leads to a uniform formulation and prevents phase separation [10].

These results showed that the encapsulation of the drug into the PBF in particles of nano-size increased the targeting efficiency and reduced the negative effects of the drug. Zeta potential is an important factor to evaluate the stability of colloidal systems [21]. In this study, the CC/PBF shifts to a positive charge by the amino group. The positive charge increases by the amino group and, the drug is placed on the nanoparticle surface and slow-released.

The abnormal changes in sex hormones have been shown in cases of underlying IVF cycle [23]. In this study, it was observed that treatment with CC caused the increased serum E2 levels as compared with the control group. This observation was on the same lines as the study conducted by Ertzeid et al., who reported the increased E2 concentrations in mice treated with CC [24]. According to these results, using Phosal for drug delivery system may have balance the impact of CC on the serum levels of hormones involved in implantation.

During the menstrual cycle in women, the estrogen and progesterone hormones cause changes at the molecular level in endometrial cells so that eventually make the endometrium ready for blastocyst acceptance and pregnancy consolidation; impairment of endometrial differentiation causes implantation failure and consequently infertility. To date, no study has reported the effects of clomiphene citrate on the genes of endometrial receptivity in mice, such as *LIF*, *LIFR*, *HOXA10*, *CSF*, *MUC1*, *progesterone receptor (PGR)*, *VEGF*, *EGF*, *FGF2*, and *HBEGF*. When the *PGR* is increased, the expression of genes involved in implantation is reduced [25]. One of the membrane mucin glycoproteins present in the uterine epithelial cell is *MUC1*. *MUC1* is highly glycosylated and acts as an anti-binding molecule on the surface of uterine epithelial cells. Based on the role and function of *MUC1* at the endometrial level, the presence or absence of this molecule in the implantation process will be important, and its overexpression inhibits embryo attachment that this gene is affected by progesterone and estrogen hormones, studies have shown a linear relationship between *MUC1*, *PGR* and endometrial receptivity [26].

Studies have shown a linear relationship between estradiol and *PGR* [27], with an increase in estradiol, *PGR* levels also increase, it may negatively affect endometrial receptivity; with an increase in *PGR*, *MUC1* levels also increase, as well as the endometrial receptivity decreases on the hand when some genes like *HOXA10*, decrease cause endometrial defectiveness and implantation failure [25]. By decreasing *HOXA10* expression, the *LIF* gene expression is also decreased [28]. With increasing estradiol, *VEGF* gene expression decreases and implantation rate decreases [29]. Since there is a linear relationship between *VEGF* and *FGF2* and *EGF* during implantation, the expression of *FGF2* and *EGF* decreases with *VEGF* depletion [30, 31]. Another study showed that with

increased estradiol levels in women undergoing IVF, *HBEGF* levels [32] and cytokines involved in implantation such as *CSF* [33] decreased and also the endometrial thickness decreased, whereas the implantation was failed.

In this study, the mRNA levels of *LIF*, *LIFR*, *HOXA10*, *HBEGF*, and *EGF* were significantly upregulated and *MUC1* and *PGR* mRNA levels were significantly downregulated in the CC-containing PBF-treated animals compared with only CC group ( $P < 0.05$ ).

Other studies showed that sirolimus and tumor-inhibiting Src kinase inhibitor TG100435, which are drugs formulated with Phosal 50PG, displayed a better overall therapeutic effect [7]. It may be considered that phospholipids can be used in the formulations of oral drugs as excipients in order to improve absorption, sustain the release and decrease the side effects [34, 35].

Foroughi et al. showed the reduced side effects of tamoxifen on endometrium when tamoxifen was loaded in palm oil lipids (S154), and soy lecithin (S100) [36]. Saesoo et al. showed the reduced side effects of cisplatin (*cis*-diamminedichloroplatinum) during a cervical usage when the cisplatin was loaded in palm oil lipids (S154), and soy lecithin (S100) [37, 38]. These lipoids include increasing the targeted effects of drugs and reducing their negative effects in non-target tissues [39, 40]. Usually, phospholipids are used to establish various carrier systems and will lead to enhance stability, solubility and successful delivery of the active pharmaceutical ingredients (API), including liposomes, micelles and some solid lipid nanoparticles (SLN) [REF]. In addition, emulsifying characteristics of phospholipids were used to assemble several drug delivery systems for oral and injection interventions [10]. The reduced side effects of CC were mainly caused due to the presence of phospholipids in these formulations.

CC/PBF in this study reduced the side effects of clomiphene citrate on endometrial tissue. In addition, the toxicity of the drug was reduced and endometrial receptivity may be improved by slow-release property. As a result, it showed that the CC-encapsulated PBF in the nano-sized positively affected the implantation-related pathways compared to the CC suspension. This finding suggests that the CC-containing PBF may be a more effective ovulation stimulation drug as compared to the CC suspension and has fewer side effects on endometrial receptivity.

## Conclusion

Sustained release formulation of clomiphene citrate increased its targeting efficiency and improved the impact of the CC on the serum levels of estradiol and expression of genes involve implantation. A new PBF has been introduced to decrease the side effect of clomiphene citrate on the endometrium; this

drug formulation could react better in implantation and preventing abortion by increasing genes involved in implantation. The development of PBF can provide possible alternatives to conventional formulations for the oral delivery of lipophilic compounds without any side effects on non-target tissues.

**Acknowledgements** We gratefully acknowledge the financial support of the Cellular and Molecular Research Center of Iran University of Medical Sciences. The study was supported by the Iran University of Medical Sciences (94-05-117-27524).

**Funding information** The Cellular and Molecular Research Center of Iran University of Medical Sciences.

## Compliance with ethical standards

**Declaration of conflicting interests** There are no other competing commercial interests.

## References

- Lai M, Ma H, Song X. Electroacupuncture combined with clomiphene promotes pregnancy and blastocyst implantation possibly by up-regulating expression of insulin receptor and insulin receptor substrate 1 proteins in endometrium in rats with PCOS. *Zhen Ci Yan Jiu*. 2016;41(5):435–9.
- Bao SH, Le Sheng S, Peng YF, De Lin Q. Effects of letrozole and clomiphene citrate on the expression of HOXA10 and integrin  $\alpha v \beta 3$  in uterine epithelium of rats. *Fertil Steril*. 2009;91(1):244–8.
- Omran E, El-Sharkawy M, El-Mazny A, Hammam M, Ramadan W, Latif D, et al. Effect of clomiphene citrate on uterine hemodynamics in women with unexplained infertility. *Int J Women's Health*. 2018;10:147–52.
- Mehdinejadi S, Amidi F, Mehdizadeh M, Barati M, Pazhohan A, Alyasin A, et al. Effects of letrozole and clomiphene citrate on Wnt signaling pathway in endometrium of polycystic ovarian syndrome and healthy women. *Biol Reprod*. 2018;100(3):641–8.
- van Hoogevest P. Review—an update on the use of oral phospholipid excipients. *Eur J Pharm Sci*. 2017;108:1–12.
- Fricker G, Kromp T, Wendel A, Blume A, Zirkel J, Rebmann H, et al. Phospholipids and lipid-based formulations in oral drug delivery. *Pharm Res*. 2010;27(8):1469–86.
- Carlson R, Hartman D, Ochalski S, Zimmerman J, Glaser K. Sirolimus (rapamycin, Rapamune®) and combination therapy with cyclosporin a in the rat developing adjuvant arthritis model: correlation with blood levels and the effects of different oral formulations. *Inflamm Res*. 1998;47(8):339–44. <https://doi.org/10.1007/s000110050339>.
- Hauss DJ. Oral lipid-based formulations. *Adv Drug Deliv Rev*. 2007;59(7):667–76.
- Khani S, Abbasi S, Keyhanfar F, Amani A. Use of artificial neural networks for analysis of the factors affecting particle size in mebudipine nanoemulsion. *J Biomol Struct Dyn*. 2019;37(12):3162–7. <https://doi.org/10.1080/07391102.2018.1510341>.
- Khani S, Keyhanfar F. Improved oral bioavailability of mebudipine upon administration in PhytoSolve and Phosal-based formulation (PBF). *AAPS PharmSciTech*. 2014;15(1):96–102. <https://doi.org/10.1208/s12249-013-0039-x>.
- Bali V, Ali M, Ali J. Study of surfactant combinations and development of a novel nanoemulsion for minimising variations in

- bioavailability of ezetimibe. *Colloids Surf B Biointerfaces*. 2010;76(2):410–20.
12. AL-Rekabi SA. Histological and hormonal study on effect of clomiphene citrate (CC) on some reproductive and embryonic parameters in female mice. *IJEIR*. 2017;7(1):7–16.
  13. Nelson LM, Hershlag A, Kurl RS, Hall JL, Stillman RJ. Clomiphene citrate directly impairs endometrial receptivity in the mouse. *Fertil Steril*. 1990;53(4):727–31.
  14. London SN, Young D, Caldito G, Mailhes JB. Clomiphene citrate-induced perturbations during meiotic maturation and cytogenetic abnormalities in mouse oocytes in vivo and in vitro. *Fertil Steril*. 2000;73(3):620–6.
  15. Smeriglio VL, Wilcox HC. Prenatal drug exposure and child outcome. *Clin Perinatol*. 1999;26(1):1–16.
  16. Amjadi F, Aflatoonian R, Javanmard SH, Saifi B, Ashrafi M, Mehdizadeh M. Apolipoprotein A1 as a novel anti-implantation biomarker in polycystic ovary syndrome: a case-control study. *J Res Med Sci*. 2015;20(11):1039–45.
  17. Salam EA, Essam ME, ElSawy NA. Effect of clomiphene citrate on the ovary of adult rat. *JOKULL*. 2015;65(12):26–44.
  18. Barnes LE, Meyer RK. Effects of ethamoxytriphetol, MRL-37, and clomiphene on reproduction in rats. *Fertil Steril*. 1962;13(5):472–80.
  19. Gadalla MA, Huang S, Wang R, Norman RJ, Abdullah SA, El Saman AM, et al. Effect of clomiphene citrate on endometrial thickness, ovulation, pregnancy and live birth in anovulatory women: systematic review and meta-analysis. *Ultrasound Obstet Gynecol*. 2018;51(1):64–76. <https://doi.org/10.1002/uog.18933>.
  20. Chen C, Yan Q, Liu K, Zhou X, Xian Y, Liang D, et al. Endometrial receptivity markers in mice stimulated with raloxifene versus clomiphene citrate and natural cycles. *Reprod Sci*. 2016;23(6):748–55.
  21. Montasser I, Fessi H, Coleman A. Atomic force microscopy imaging of novel type of polymeric colloidal nanostructures. *Eur J Pharm Biopharm*. 2002;54(3):281–4.
  22. Patel MH, Mundada VP, Sawant KK. Novel drug delivery approach via self-microemulsifying drug delivery system for enhancing Oral bioavailability of Asenapine maleate: optimization, characterization, cell uptake, and in vivo pharmacokinetic studies. *AAPS PharmSciTech*. 2019;20(2):44.
  23. Bocca S, Real EB, Lynch S, Stadtmayer L, Beydoun H, Mayer J, et al. Impact of serum estradiol levels on the implantation rate of cleavage stage cryopreserved-thawed embryos transferred in programmed cycles with exogenous hormonal replacement. *J Assist Reprod Genet*. 2015;32(3):395–400.
  24. Ertzeid G, Storeng R. The impact of ovarian stimulation on implantation and fetal development in mice. *Hum Reprod*. 2001;16(2):221–5.
  25. Lee B, Du H, Taylor HS. Experimental murine endometriosis induces DNA methylation and altered gene expression in eutopic endometrium. *Biol Reprod*. 2009;80(1):79–85. <https://doi.org/10.1095/biolreprod.108.070391>.
  26. Aplin JD, Meseguer M, Simon C, Ortiz ME, Croxatto H, Jones CJ. MUC1, glycans and the cell-surface barrier to embryo implantation. *Biochem Soc Trans*. 2001;29(Pt 2):153–6. <https://doi.org/10.1042/0300-5127:0290153>.
  27. Dixon D, He H, Haseman JK. Immunohistochemical localization of growth factors and their receptors in uterine leiomyomas and matched myometrium. *Environ Health Perspect*. 2000;108(Suppl 5):795–802.
  28. Chen CR, Yan QX, Zhou XQ, Xian YJ, Guo XY, Quan S. Effects of raloxifene at two different doses for ovulation induction on endometrial pinopodes in mice during the implantation window. *Nan Fang Yi Ke Da Xue Xue Bao*. 2018;38(2):234–8.
  29. Mueller MD, Vigne JL, Minchenko A, Lebovic DI, Leitman DC, Taylor RN. Regulation of vascular endothelial growth factor (VEGF) gene transcription by estrogen receptors alpha and beta. *Proc Natl Acad Sci U S A*. 2000;97(20):10972–7. <https://doi.org/10.1073/pnas.200377097>.
  30. Seghezzi G, Patel S, Ren CJ, Gualandris A, Pintucci G, Robbins ES, et al. Fibroblast growth factor-2 (FGF-2) induces vascular endothelial growth factor (VEGF) expression in the endothelial cells of forming capillaries: an autocrine mechanism contributing to angiogenesis. *J Cell Biol*. 1998;141(7):1659–73. <https://doi.org/10.1083/jcb.141.7.1659>.
  31. Moller B, Rasmussen C, Lindblom B, Olovsson M. Expression of the angiogenic growth factors VEGF, FGF-2, EGF and their receptors in normal human endometrium during the menstrual cycle. *Mol Hum Reprod*. 2001;7(1):65–72. <https://doi.org/10.1093/molehr/7.1.65>.
  32. Wang H, Shi G, Li M, Fan H, Ma H, Sheng L. Correlation of IL-1 and HB-EGF with endometrial receptivity. *Exp Ther Med*. 2018;16(6):5130–6. <https://doi.org/10.3892/etm.2018.6840>.
  33. Kumar P, Mahajan S. Preimplantation and postimplantation therapy for the treatment of reproductive failure. *J Hum Reprod Sci*. 2013;6(2):88–92. <https://doi.org/10.4103/0974-1208.117165>.
  34. Lanza FL, Marathi UK, Anand BS, Lichtenberger LM. Clinical trial: comparison of ibuprofen-phosphatidylcholine and ibuprofen on the gastrointestinal safety and analgesic efficacy in osteoarthritic patients. *Aliment Pharmacol Ther*. 2008;28(4):431–42. <https://doi.org/10.1111/j.1365-2036.2008.03765.x>.
  35. Semalty A, Semalty M, Singh D, Rawat MS. Development and physicochemical evaluation of pharmacosomes of diclofenac. *Acta Pharma*. 2009;59(3):335–44. <https://doi.org/10.2478/v10007-009-0023-x>.
  36. Foroughi S, Ziamajidi N, Javid S, Abbasalipourkabir R, Aflatoonian R, Ashrafi M, et al. Study of telomerase reverse transcriptase and uterine-ovarian-specific genes expression in the endometrial tissue of ovariectomized female Sprague-Dawley rats. *Int J Biol Macromol*. 2018;113:1302–7. <https://doi.org/10.1016/j.ijbiomac.2018.02.115>.
  37. Saesoo S, Bunthot S, Sajomsang W, Gonil P, Phunpee S, Songkhum P, et al. Phospholipid-chitosan hybrid nanoliposomes promoting cell entry for drug delivery against cervical cancer. *J Colloid Interface Sci*. 2016;480:240–8. <https://doi.org/10.1016/j.jcis.2016.06.071>.
  38. Ma Y, Zhao X, Li J, Shen Q. The comparison of different daidzein-PLGA nanoparticles in increasing its oral bioavailability. *Int J Nanomedicine*. 2012;7:559–70. <https://doi.org/10.2147/ijn.s27641>.
  39. Sriraman SK, Salzano G, Sarisozen C, Torchilin V. Anti-cancer activity of doxorubicin-loaded liposomes co-modified with transferrin and folic acid. *Eur J Pharm Biopharm*. 2016;105:40–9.
  40. Julius JM, Tanyi JL, Noguera-Gonzalez GM, Watkins JL, Coleman RL, Wolf JK, et al. Evaluation of pegylated liposomal doxorubicin dose on the adverse drug event profile and outcomes in treatment of recurrent endometrial cancer. *Int J Gynecol Cancer*. 2013;23(2):348–54. <https://doi.org/10.1097/IGC.0b013e31827c18f3>.

**Publisher's note** Springer Nature remains neutral with regard to jurisdictional claims in published maps and institutional affiliations.